PREPRINT AND PEER-REVIEW STATUS

This manuscript is a non-peer-reviewed preprint submitted to EarthArXiv. It has not yet been submitted to a journal. Subsequent versions of this manuscript may have slightly different content and will note the journal submission. If accepted, the final version of this manuscript will be available via the 'Peer-reviewed Publication DOI' link on the right-hand side of this webpage.

Do typhoons pull Indonesian smoke into the Pacific? A pre-registered test, and the record 2026 season

Author name: Lik Ren, Tai
Affiliation: Woosong University, Daejeon, Korea
Email address: likrentai@gmail.com
University email address: likrentai@wsu.ac.kr
ORCID: https://orcid.org/0009-0002-6667-3331

Do typhoons pull Indonesian smoke into the Pacific? A pre-registered test, and the record 2026 season

Lik Ren Tai*

Woosong University, Daejeon, Korea (ORCID iD: 0009-0002-6667-3331)
Corresponding author: likrentai@gmail.com

Abstract

In August to October 2026, during an El Niño with the highest Oceanic Niño Index for those months since 1950 (+2.46 °C), smoke from Indonesian fires spread over the western North Pacific while an active typhoon season was under way. Since 2012, typhoons have been described as drawing Maritime Continent smoke into the monsoon flow and out over the ocean, but this rests on case studies and field campaigns. Using open satellite, reanalysis, fire and ground data, and fixing the criteria of every test in writing before computation, this study asks whether typhoons robustly increase smoke export, whether 2026 was exceptional in the typhoon zone, and why. A typhoon-day increase in smoke inflow to a corridor east of the Philippines (128 to 150° E, 3 to 18° N), found in MERRA-2 for 2003 to 2026, failed a placebo test ($p = 0.105$) and did not replicate in 23 independent seasons (1980 to 2002). In the same corridor, August to October 2026 had the highest aerosol optical depth (AOD) of the VIIRS era (2012 to 2026) in both VIIRS satellites, 8% above 2015 in VIIRS SNPP. The lead was 21% for August to September, and 2026 ranked first in August and in September separately, while 2015 peaked in October. The excess was fine-mode smoke, and AERONET stations at the source confirmed 2026 above 2015. Fire radiative power over Indonesia as a whole was 29% lower than in 2015, but in eastern Indonesia, the source nearest the corridor, it was the highest of the period and three times the 2015 value in August. Winds and rainfall favoured the corridor, but no more than in 2015. The 2026 record reflects where and when Indonesia burned, not a typhoon effect on export.

Keywords: Biomass burning; Smoke transport; Aerosol optical depth; Tropical cyclones; El Niño; Maritime Continent; Pre-registration

1. Introduction

1.1 Background

Fires in Indonesia's peatlands and forests produce some of the largest smoke episodes on Earth. Burning peaks from August to October and is strongly modulated by El Niño, which lengthens the dry season and lowers peat water tables (Page et al. 2002; Field et al. 2016). Burning is closely tied to rainfall deficits, and its sensitivity to drought has been amplified by land-use change (Field et al. 2009; Fanin and van der Werf 2017). The 1997 and 2015 seasons were the largest of recent decades (van der Werf et al. 2017), and fire carbon emissions in 2015 were the highest since 1997 (Huijnen et al. 2016). The resulting haze carries large health burdens across Equatorial Asia (Marlier et al. 2013; Koplitz et al. 2016; Crippa et al. 2016). Most attention has gone to the haze

over Sumatra, Kalimantan, Singapore and Malaysia, where exposure is greatest; smoke carried north and east into the western North Pacific has received less.

In boreal summer and autumn, the Maritime Continent lies under the southwest monsoon, next to the most active tropical cyclone basin on Earth. El Niño shifts typhoon formation south-eastward and favours longer-lived and more intense storms (Chan 1985; Wang and Chan 2002; Camargo and Sobel 2005), and the Madden–Julian Oscillation modulates when they form (Madden and Julian 1971; Maloney and Hartmann 2001). Since 2012, work by the U.S. Naval Research Laboratory and colleagues has described how western North Pacific tropical cyclones interact with Maritime Continent smoke: their inflow can accelerate the monsoon flow and draw smoke north and east, while their rain can scavenge it (Reid et al. 2012, 2015, 2016a, 2016b, 2023; Hilario et al. 2021). These descriptions rest on conceptual analyses, case studies, cruises and field campaigns. Modelling of single events supports them; in October 2006, Typhoon Xangsane carried Sumatran smoke eastward below 700 hPa (Wang et al. 2013). Climatologies of smoke transport pathways, however, have not been conditioned on typhoons (Xian et al. 2013), and the typhoon effect on smoke export has not, to my knowledge, been tested statistically over many seasons. Observation is part of the difficulty: persistent cloud limits satellite views of the region's aerosol (Reid et al. 2013).

The 2026 fire season gave the question new weight. A strong El Niño developed through the northern summer, with the Oceanic Niño Index reaching +2.46 °C for August to October, the highest for those months since records began in 1950, and Indonesian fire emissions in August were reported to be the highest for that month since at least 2003 (Shetty 2026). Haze reached Luzon on 1 September (Daily Tribune 2026) and northern Mindanao by late September, and hazardous levels were recorded in Zamboanga City on 15 October (Echeminada 2026; Inquirer 2026). The western North Pacific meanwhile had an active season with several intense typhoons, including Super Typhoons Choi-wan and Champi. In late September and early October, a streamer of smoke reached from eastern Indonesia towards the outer circulation of Choi-wan east of the Philippines, and public commentary during the season named typhoons among the factors behind the regional haze (The Straits Times 2026).

1.2 Aim and contribution

This study asks three questions. First, do typhoons robustly increase smoke export into the typhoon zone east of the Philippines, as the conceptual picture suggests? Second, was August to October 2026 exceptional for smoke in that zone, judged by independent satellite observations rather than a single model? Third, if so, what set it apart: more burning, transport more favourable to the zone, or less rain on the way?

The study began from an exploratory analysis of 2026 that suggested both a record and a typhoon effect. Because such a starting point invites finding what one is looking for, each question was then answered by a test whose data, metric, pass criteria and decision rule were written down before any computation, with later changes recorded as dated amendments and both versions reported. This follows the logic of pre-registration (Nosek et al. 2018) and responds to the concern that statistical results in atmospheric science are often overstated (Wilks 2016). Placebo tests, leave-one-season-out checks and replication on independent years were

part of the criteria. The author works in applied data science rather than atmospheric science; the procedure is meant to make every step open to checking, and the analysis code and the dated criteria are published with the paper.

The contributions are (i) a negative result for typhoon-driven export: the mechanism, real in individual events, does not leave a robust signature in daily export statistics; (ii) an observational record claim for 2026 in the typhoon zone, bounded by what the satellites can support; and (iii) evidence that the record came from the location and timing of burning rather than its total.

2. Study area

The study covers the Maritime Continent and the western North Pacific between 94 and 160° E and 12° S and 25° N (Fig. 1). The **Pacific corridor** (128 to 150° E, 3 to 18° N) is the open ocean east of the Philippines through which many western North Pacific typhoons pass, and is the receptor region. The **eastern Indonesia** region (119 to 141° E, 9° S to 2° N; Sulawesi, Maluku and Papua) is the fire source nearest to the corridor; Sumatra and Kalimantan, the largest sources in most years, lie 1,500 to 3,000 km further west. A **gateway** band (125 to 141° E, 2° S to 3° N) between the two is used to describe the low-level flow towards the corridor. Typhoon days are defined by storms inside 120 to 150° E, 5 to 25° N. From August to October the low-level flow over the region is the southwest monsoon, and the corridor lies at the eastern end of the monsoon trough, where many typhoons form.

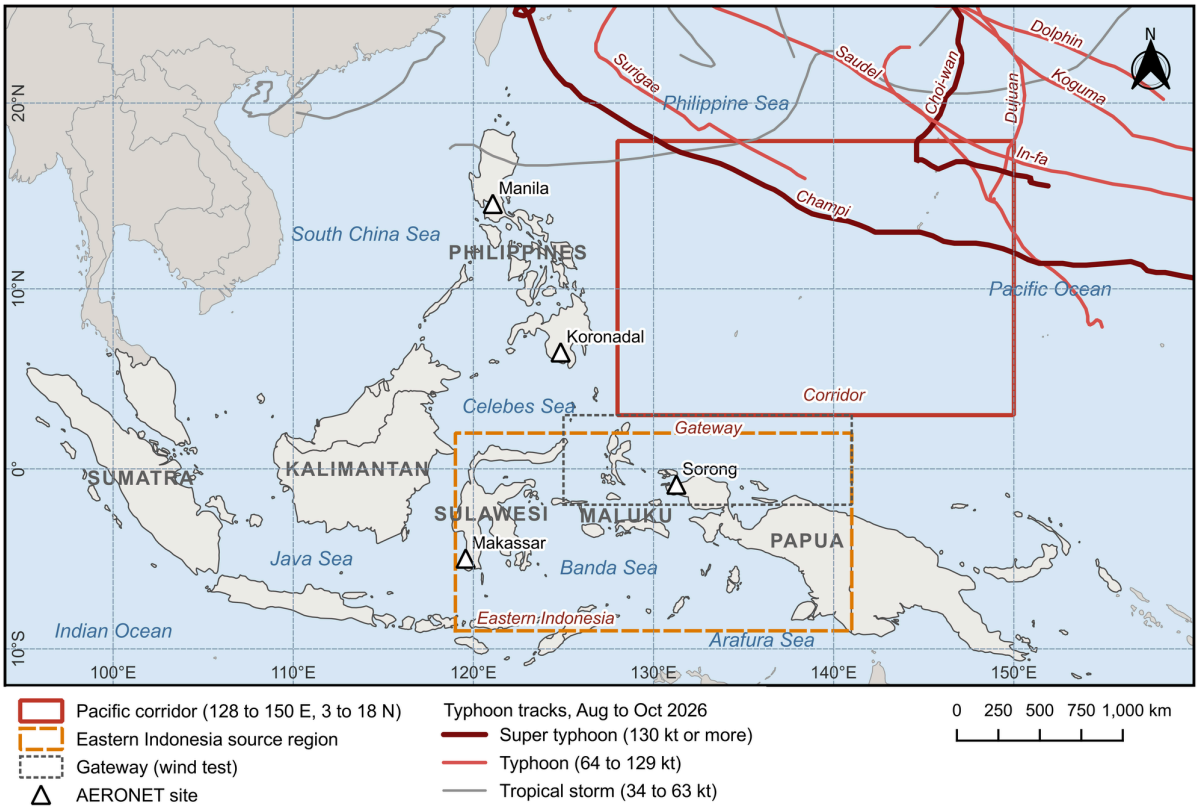


Figure 1. *Study area: the Pacific corridor (receptor), the eastern Indonesia source region and the gateway band, with the four AERONET sites used in the ground check and the tracks of the tropical storms and typhoons of August to October 2026 (IBTrACS), shaded by peak intensity; names are given for typhoons (64 kt or more).*

3. Data and methods

3.1 Data

All data are open (Table S1). Aerosol optical depth (AOD) at 550 nm comes from the VIIRS Deep Blue Level 3 daily products at 1° (Hsu et al. 2019; Sayer et al. 2018, 2019) on two satellites, Suomi NPP (SNPP, 2012 onwards) and NOAA-20 (2018 onwards); the Ångström exponent and the fine-mode fraction over the ocean from the same files serve as smoke indicators, since fine smoke particles raise both relative to sea salt (Eck et al. 1999). MODIS Aqua Collection 6.1, combined Dark Target and Deep Blue (Levy et al. 2013), extends the record to 2002. Smoke mass and fluxes come from the MERRA-2 aerosol reanalysis (Gelaro et al. 2017; Randles et al. 2017; Buchard et al. 2017) for 1980 to 2026, with smoke defined as organic plus black carbon. Fire activity is the fire radiative power (FRP) of the VIIRS 375 m active fire detections distributed by FIRMS (Schroeder et al. 2014), summed per 0.5° cell and day; FRP scales with the rate at which biomass is burned (Wooster et al. 2005), with GFAS emissions (Kaiser et al. 2012) as a secondary record. Winds at 850 and 700 hPa and rainfall are ERA5 monthly means (Hersbach et al. 2020). Ground-based AOD is AERONET version 3, Level 1.5 (Giles et al. 2019; Holben et al. 1998). Typhoon tracks are IBTrACS v04r01 (Knapp et al. 2010), using the U.S. agency maximum sustained wind, and the Madden–Julian Oscillation (MJO) is described by the RMM index (Wheeler and Hendon 2004). The season is 1 August to 31 October unless stated otherwise.

Three data-version issues were settled before the tests that depend on them. NASA serves VIIRS Deep Blue version 2 for 2012 to 2025 and version 2.1 from mid-June 2026. Version 2 exists for all of August to October 2026 except 30 and 31 October, which had not yet been processed, so version 2 was used throughout; on 60 days with both versions, corridor AOD differs by −1.5% (SNPP) and −1.2% (NOAA-20), with a daily correlation of 1.000. FIRMS data are standard processing for 2012 to 2025 but near-real-time for 2026; the step between them will be checked when standard data for 2026 are released. GFAS changes from the MODIS-based version 1.2 to the VIIRS-based version 1.4.2 on 1 January 2026, without overlap, so GFAS is not used for any comparison across that date.

3.2 Pre-registered tests

The analysis is a sequence of tests (Table 1). For each, a criteria document recorded, before any computation, the question, data and metric, the deciding checks with their pass levels, a decision rule stating what the paper would claim for each outcome, and quantities to be reported without deciding anything. What was already known when the criteria were written is disclosed in each document. Changes after agreement are listed with dates and reasons in Supplementary Section S1; none altered a pass level after results were seen. Tests 2, 3, 3d, 4 and 6 were run twice, in a cloud environment and on a desktop computer, with identical results; Tests 2b and 3c and the data downloads were run on the desktop computer only.

3.3 Typhoons and smoke export (Tests 2 and 2b)

The exploratory analysis measured smoke inflow in MERRA-2 (the column flux of organic plus black carbon, in t per day) through the southern side of the corridor. A typhoon day was a day with at least one storm of 64 kt or more inside 120 to 150° E, 5 to 25° N. Daily inflow was expressed as departures from a centred 15-day running mean within each season, and the typhoon effect as the mean departure on typhoon days minus that on other days, over August to October 2003 to 2026 (495 typhoon days), with 95% intervals from a bootstrap over seasons (Efron and Tibshirani 1993).

Test 2 asked whether this effect is robust. Its deciding checks were (C1) a placebo in which each season's series of typhoon days was shifted circularly by a random offset, 1,000 times, keeping the clustering of typhoon days, with the observed effect required to exceed the 97.5th percentile of the shifted effects; (C2) 36 variants of intensity threshold (34, 50 and 64 kt), typhoon box and baseline, of which at least 29 had to be positive and 18 clearly so; (C3) leaving out each season in turn; and (C4) control for the MJO by estimating the effect within RMM phases. Test 2b took the pattern suggested by the exploratory analysis, a pulse of inflow on the day a typhoon enters the box and the day after, followed by a deficit three to four days later, and tested it with the same placebo method on 111 typhoon entries in 23 earlier seasons (1980 to 2002) that had not been examined. The Choi-wan case (Section 4.1) uses 3-hourly near-surface smoke (organic, brown and black carbon) from the GEOS-FP forecast system and forward trajectories in ERA5 winds at 850 hPa, released every 6 h from 28 September to 4 October from each 0.5° cell in eastern Indonesia with at least 10 VIIRS hotspots that day and followed for 144 h; a parcel reached the storm if it came within 500 km of its centre.

3.4 The 2026 record and its timing (Tests 3, 3c and 3d)

The record metric is the mean AOD over all valid 1° cell-days in the corridor, weighted by the cosine of latitude and computed identically for every season. A season is ranked only if at least 30% of its corridor cell-days have a valid retrieval (O0). The record check (O1) required 2026 to rank first in both VIIRS records, and the firmness of the rank was assessed by resampling the days of every season 2,000 times. Test 3 used August to September, the period available in MERRA-2 when it was designed; Test 3c extended it to August to October. Test 3d ranked August and September separately (T1) and compared the date on which each season reached half of its August to October total (T2); days without retrievals took the season's own mean. MODIS Aqua was used to ask whether the record extends back to 2002.

3.5 Burning, transport and rain (Test 4)

Test 4 compared 2026 with all seasons on three candidate drivers. Burning was the mean daily FRP summed over Indonesian 0.5° cells, and over the Indonesian cells of the eastern region; a cell counted as Indonesian if, sampled at 5 × 5 points, it held at least as much Indonesian land as land of any other country. Days without any detection in the whole download area were treated as satellite outages, not as days without fire. Transport was the mean northward wind at 850 hPa over the gateway band, and rain the mean rainfall over the corridor. The deciding checks were a burning record in both VIIRS records and both regions (B1), eastern burning at least equal to 2015 (B2), a northward wind among the three strongest seasons (T1), and a corridor among the three driest (D1). The test is descriptive; it does not apportion the record between drivers.

3.6 Ground check (Test 6)

No AERONET site inside the corridor has data for these seasons, so Test 6 used the four nearest sites that do: Koronadal (ND Marbel University, Mindanao), Manila, Sorong (West Papua) and Makassar (Sulawesi). AERONET AOD at 500 nm was converted to 550 nm with each site's 440 to 870 nm Ångström exponent and compared with VIIRS SNPP in the 1° cell containing the site on the same days. VIIRS was required to correlate with AERONET at r of at least 0.6 at three sites (G1), and AERONET and VIIRS together to place 2026 above 2015 at most sites with at least 20 days in both years (G2).

3.7 Model comparison

MERRA-2 AOD was averaged to the VIIRS grid and sampled on the cell-days with valid VIIRS retrievals; agreement in the ranking of seasons was required at a Spearman correlation of at least 0.7 (O2). This check qualifies how MERRA-2 rankings may be used; it does not decide the record.

4. Results

Table 1 summarises the outcome of every test; the main quantities for 2015 and 2026 are compared in Table 2.

Table 1. *Pre-registered tests, their deciding checks and outcomes. Pass levels and decision rules were fixed before computation.*

Test	Question	Data	Deciding checks	Result	Outcome

2	Is the typhoon-day increase in corridor smoke inflow robust?	MERRA-2, 2003 to 2026	C1 placebo; C2 36 variants; C3 leave one season out; C4 MJO	+158 t per day; placebo p = 0.105; 14 of 36 variants clear; C3, C4 pass	Fail: claim dropped
2b	Does the entry pulse and deficit replicate in unseen years?	MERRA-2, 1980 to 2002 (111 entries)	D1 pulse, D2 deficit, each against placebo	Pulse +108 (cut-off +281); deficit −66 (cut-off −253)	Fail: not replicated
3	Is the 2026 corridor record seen by satellites (Aug to Sep)?	VIIRS SNPP and NOAA-20, 2012 to 2026	O0 coverage; O1 first in both; O2 MERRA-2 ranks	First in both, 21% above the next season; O2 Spearman 0.65	Pass, since 2012
3c	Does the record hold for Aug to Oct?	VIIRS; MODIS Aqua 2002 to 2025	As Test 3; MODIS rule for 2002	First in both, 8% above 2015; MODIS rule fails	Pass, narrowly over 2015
3d	Did the 2026 smoke arrive earlier than in 2015?	VIIRS, by month	T1 first in Aug and Sep; T2 half-season date	First in Aug and Sep in both; 19 Sep against 27 Sep	Pass
4	More burning, transport or less rain?	FIRMS FRP; ERA5	B1 burning record; B2 east ≥ 2015; T1 wind top three; D1 rain driest three	Indonesia 2nd (0.71 of 2015); east 1st (1.14); wind 3rd; rain 2nd driest	B1 fails; B2, T1, D1 pass
6	Do ground stations agree with VIIRS?	AERONET Level 1.5, four sites	G1 r ≥ 0.6 at three sites; G2 2026 above 2015	r = 0.81 to 0.96 at three sites; 2026 above 2015 at three of four	Pass

Criteria, amendments and full results are in Supplementary Section S1. Test 1 was the literature search summarised in Section 1.1; Test 5, a request for outside review, is not an analysis. Checks to be rerun when data are released: O2 and Test 2 with MERRA-2 October 2026; Test 4 with standard FIRMS data for 2026.

4.1 Typhoons and smoke export

In MERRA-2, smoke inflow to the corridor on typhoon days exceeded that on other days by 158 t per day (29%) over 2003 to 2026. The effect was positive in all 24 leave-one-season-out samples and kept its size within MJO phases (103%), but it failed the placebo: randomly shifted typhoon calendars gave effects at least as large in 10.5% of cases (p = 0.105; Fig. 2a), and it was clearly positive in only 14 of 36 variants (Fig. S1). It was concentrated in El Niño seasons (+430 t per day) and absent in others (+19). The typhoon-day effect is therefore not distinguishable from the timing of typhoons within smoky seasons. The pulse-and-deficit pattern around typhoon entries did not replicate in 1980 to 2002: the pulse was +108 t per day against a placebo 97.5th percentile of +281, and the deficit −66 against a 2.5th percentile of −253 (Fig. 2b). A broad shape, higher inflow before typhoon days than after, recurred, but part of it may be produced by the running-mean baseline itself.

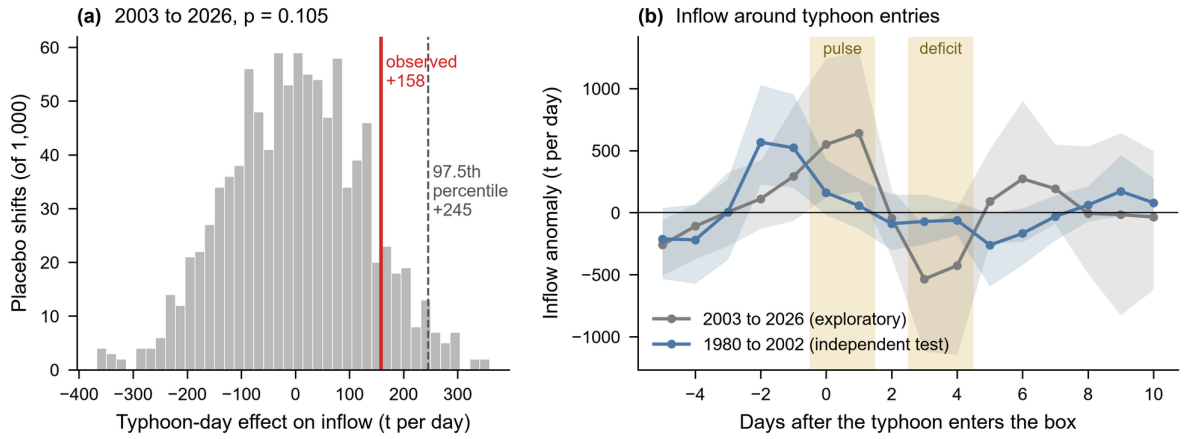


Figure 2. *Typhoons and smoke inflow to the corridor (MERRA-2): (a) distribution of the typhoon-day effect under 1,000 placebo shifts of the typhoon calendar, 2003 to 2026, with the observed effect (+158 t per day) and the 97.5th percentile of the placebo effects (+245); (b) inflow anomaly around typhoon entries into the box in the exploratory seasons 2003 to 2026 and the independent seasons 1980 to 2002, with 95% bands from resampling seasons; shaded columns mark the pre-registered pulse (days 0 and +1) and deficit (days +3 and +4) windows.*

Individual events can still be striking. During Super Typhoon Choi-wan (30 September to 7 October 2026, peak 134 kt), the smoke-covered area of the corridor in GEOS-FP grew from 1.1 to 2.7 million km², and the smoke edge came within about 200 km of the storm centre. On 6 October, when that area peaked, a grey-brown streamer was visible in true-colour imagery from northern Papua north-eastward into the corridor, VIIRS retrieved its highest AOD over Maluku and Papua, and GEOS-FP placed the plume in the same position (Fig. 3a to c). Of air parcels released at 850 hPa over eastern Indonesia and followed forward in ERA5 winds, 47% reached the corridor but fewer than 2% the storm itself (Fig. 3d). Such streamers are visible and real, but over many seasons they do not add up to a robust typhoon-day increase in export.

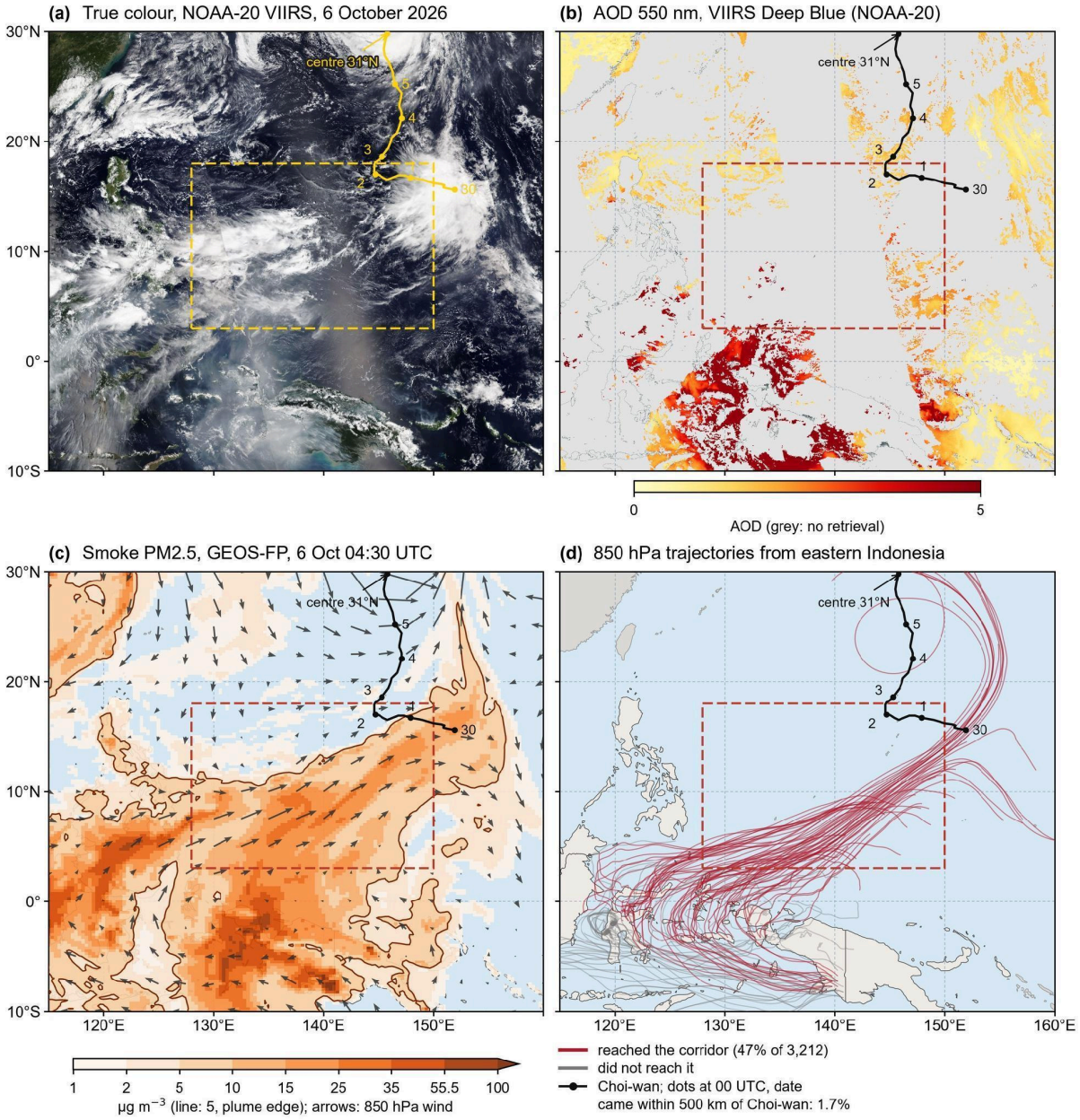


Figure 3. *Super Typhoon Choi-wan and the smoke streamer from eastern Indonesia, 6 October 2026: (a) true colour and (b) AOD at 550 nm from VIIRS Deep Blue version 2.1 (grey: no retrieval), both NOAA-20 and from NASA Worldview; (c) near-surface smoke PM2.5 (organic, brown and black carbon; GEOS-FP, 04:30 UTC), with the 5 μg m⁻³ plume edge and the 850 hPa wind (ERA5, 06:00 UTC); (d) forward trajectories at 850 hPa from eastern Indonesian fire cells, released every 6 h from 28 September to 4 October and followed for 144 h (150 of 3,212 drawn). The track of Choi-wan (IBTrACS, provisional) is marked at 00 UTC each day with the date; on 6 October its centre was near 31° N, north of the maps. Dashed box: the Pacific corridor.*

4.2 An exceptional season in the typhoon zone

August to October 2026 had the highest corridor AOD of the VIIRS era in both records: 0.221 in SNPP, against 0.204 in 2015 and 0.152 in 2012 and 2013, and 0.218 in NOAA-20, against 0.144 in 2023 (Table 2; Fig. 4). All seasons passed the coverage rule (2026: 44.5% of cell-days). The excess was smoke rather than sea salt: 2026 also had the highest Ångström exponent (SNPP 0.715, NOAA-20 0.771) and the highest fine-mode fraction

over the ocean (0.455 and 0.479) of any season in either record. In eastern Indonesia itself, 2026 AOD (0.528) was 63% above 2015 (0.323).

Table 2. *August to October 2015 and 2026 compared. Ranks are among the 15 seasons 2012 to 2026.*

Quantity	2015	2026	2026 / 2015	Rank of 2026	Source
Corridor AOD, Aug to Sep	0.170	0.205	1.21	1	VIIRS SNPP
Corridor AOD, Aug to Oct	0.204	0.221	1.08	1	VIIRS SNPP
Corridor AOD, August	0.151	0.196	1.30	1	VIIRS SNPP
Corridor AOD, October	0.260	0.245	0.94	2	VIIRS SNPP
Corridor Ångström exponent	0.641	0.715	1.12	1	VIIRS SNPP
Eastern Indonesia AOD	0.323	0.528	1.63	1	VIIRS SNPP
FRP, Indonesia (MW)	58,816	42,008	0.71	2	FIRMS SNPP
FRP, eastern Indonesia (MW)	9,803	11,173	1.14	1	FIRMS SNPP
FRP, eastern Indonesia, August (MW)	2,427	7,225	2.98	1	FIRMS SNPP
Northward wind, 850 hPa, gateway (m s^{-1})	1.73	1.46		3	ERA5
Corridor rainfall (mm per day)	7.2	7.8		2 (driest)	ERA5

FRP: mean daily fire radiative power summed over the region; outage days excluded. Wind and rainfall: mean of the three monthly means (ERA5).

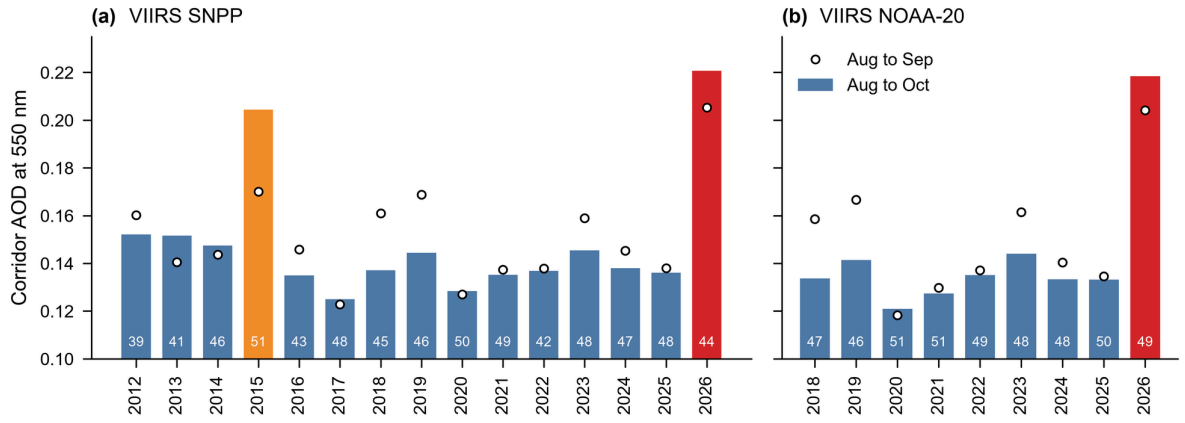


Figure 4. *Mean corridor AOD at 550 nm by season, August to October (bars) and August to September (dots): (a) VIIRS SNPP, 2012 to 2026; (b) VIIRS NOAA-20, 2018 to 2026. Numbers in the bars give the percentage of corridor cell-days with a valid retrieval, August to October; 2026 in red, 2015 in orange.*

The 2026 anomaly extended from eastern Indonesia north and north-east across the Celebes Sea into the corridor, whereas the 2015 anomaly was largest further west, over Kalimantan, Sumatra and the seas between them (Fig. 5).

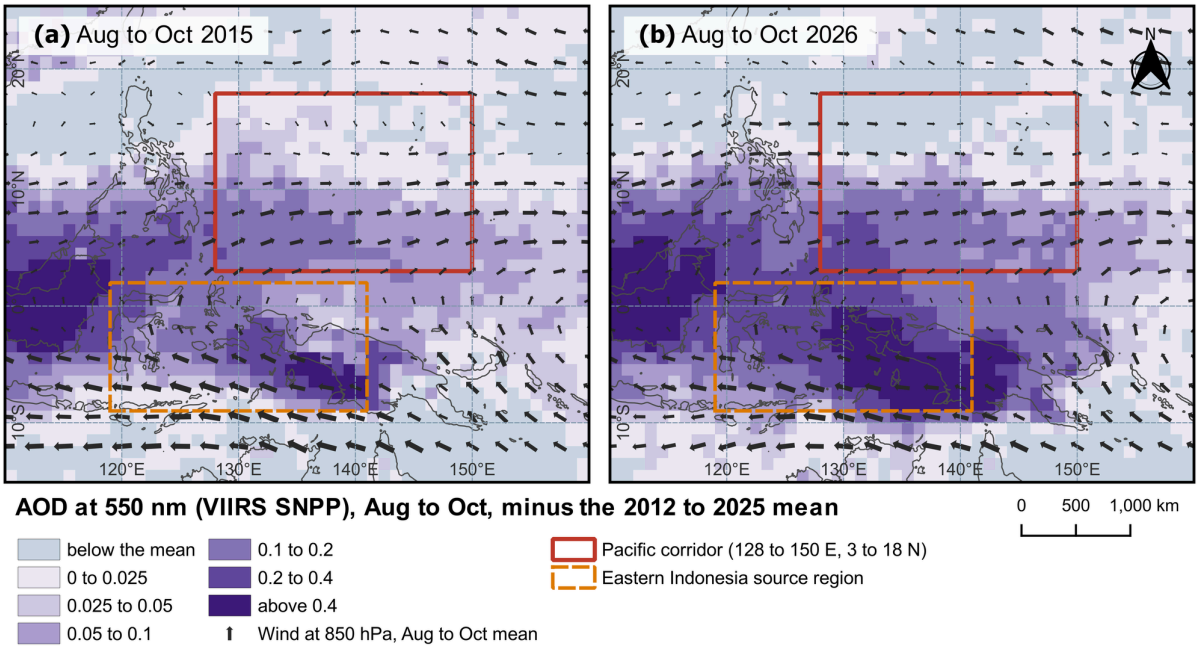


Figure 5. *AOD at 550 nm (VIIRS SNPP), August to October, minus the 2012 to 2025 mean: (a) 2015; (b) 2026. Arrows show the mean wind at 850 hPa for the same months (ERA5); boxes mark the corridor and the eastern Indonesia source region.*

The margin over 2015 depends on where the season ends. For August to September the 2026 lead was 21% in SNPP (0.205 against 0.170), and 2026 ranked first in 99.95% of day resamples; for August to October the lead was 8%, and 2026 ranked first in 86% of resamples. NOAA-20 began in 2018 and cannot check 2015. MODIS Aqua, whose orbit had drifted to a later overpass time by 2026, placed 2015 above 2026 for August to October (0.204 against 0.185; Fig. S2). MODIS coverage of the corridor is low (26 to 38% of cell-days per season), and the rule that 2015 and 2019 should be the two highest MODIS seasons of 2002 to 2025 failed, so the record claim is restricted to the VIIRS era, since 2012.

4.3 Earlier in the season

Ranked month by month, 2026 was first in August (SNPP 0.196, against 0.171 in 2019) and in September (0.212, against 0.188 in 2015) in both VIIRS records, while 2015 was first in October (0.260, against 0.245 in 2026; Fig. 6). In August, 2015 ranked only seventh. The 2026 season reached half of its total on 19 September, eight days before 2015 (27 September), although later than the median season (about 15 September), because 2026 stayed high into October. Both checks of Test 3d passed. What distinguishes 2026 is not an early peak but that the corridor was already far above every other season in August, before the 2015 smoke would have arrived.

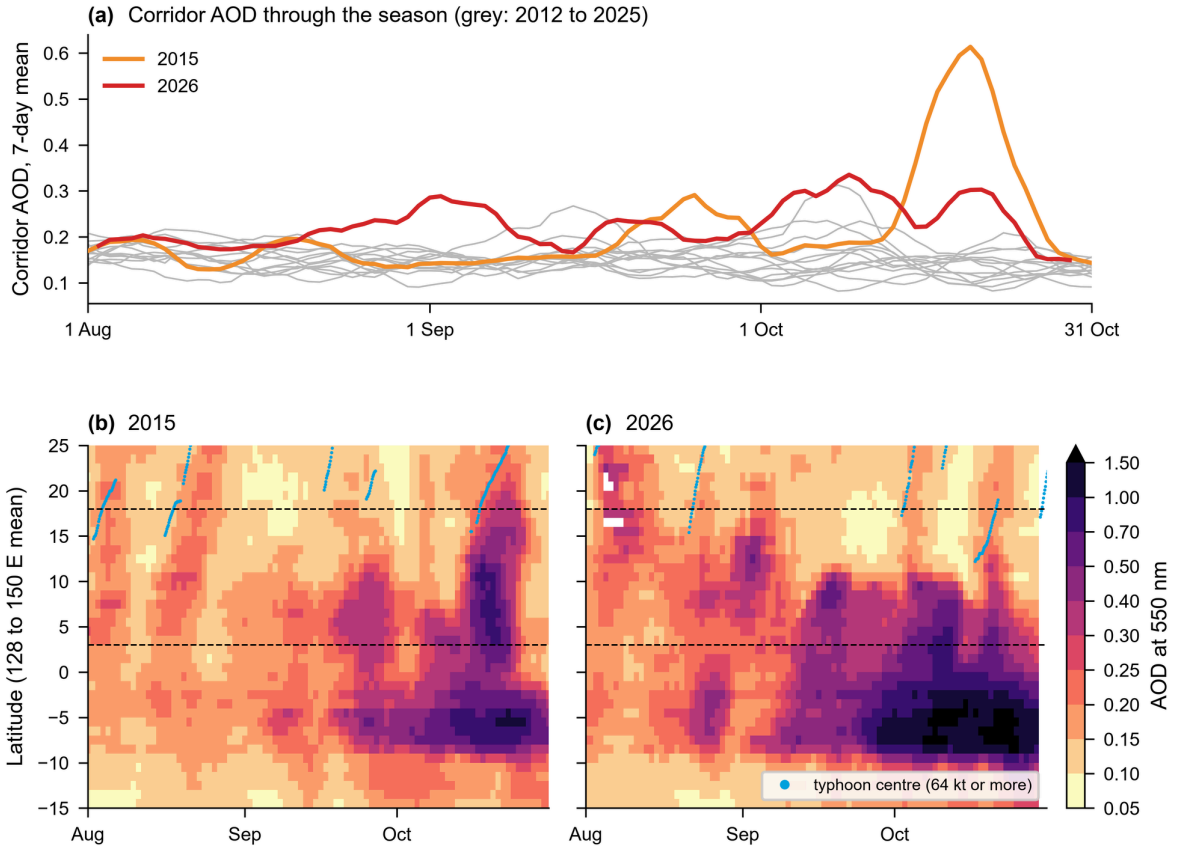


Figure 6. *Timing of the corridor smoke: (a) seven-day mean of daily corridor AOD (VIIRS SNPP) from 1 August to 31 October, 2026 and 2015 against 2012 to 2025 (grey); (b, c) latitude–time (Hovmöller) diagrams of daily AOD averaged over 128 to 150° E (five-day running mean) for (b) 2015 and (c) 2026, with the centres of typhoons (64 kt or more) in that band; dashed lines mark the latitudes of the corridor (3 and 18° N).*

4.4 Where and when Indonesia burned

Over Indonesia as a whole, 2026 was the second-largest fire season of the VIIRS era by FRP, at 71% of 2015 (mean daily FRP 42,000 against 58,800 MW in SNPP; Table 2; Fig. 7), so the burning-record check (B1) failed. In eastern Indonesia, however, 2026 burning was the largest of the period in both records, 14% above 2015 over the season (B2 passed) and three times the 2015 value in August (7,200 against 2,400 MW). Eastern Indonesia burned from the start of the 2026 season, whereas in 2015 its burning, like that in Sumatra and Kalimantan, rose through September and peaked in October (Fig. 8a, b). About 45% of eastern Indonesian FRP in 2026 came from north of 5° S (Sulawesi, Maluku and northern Papua) and 55% from southern Papua.

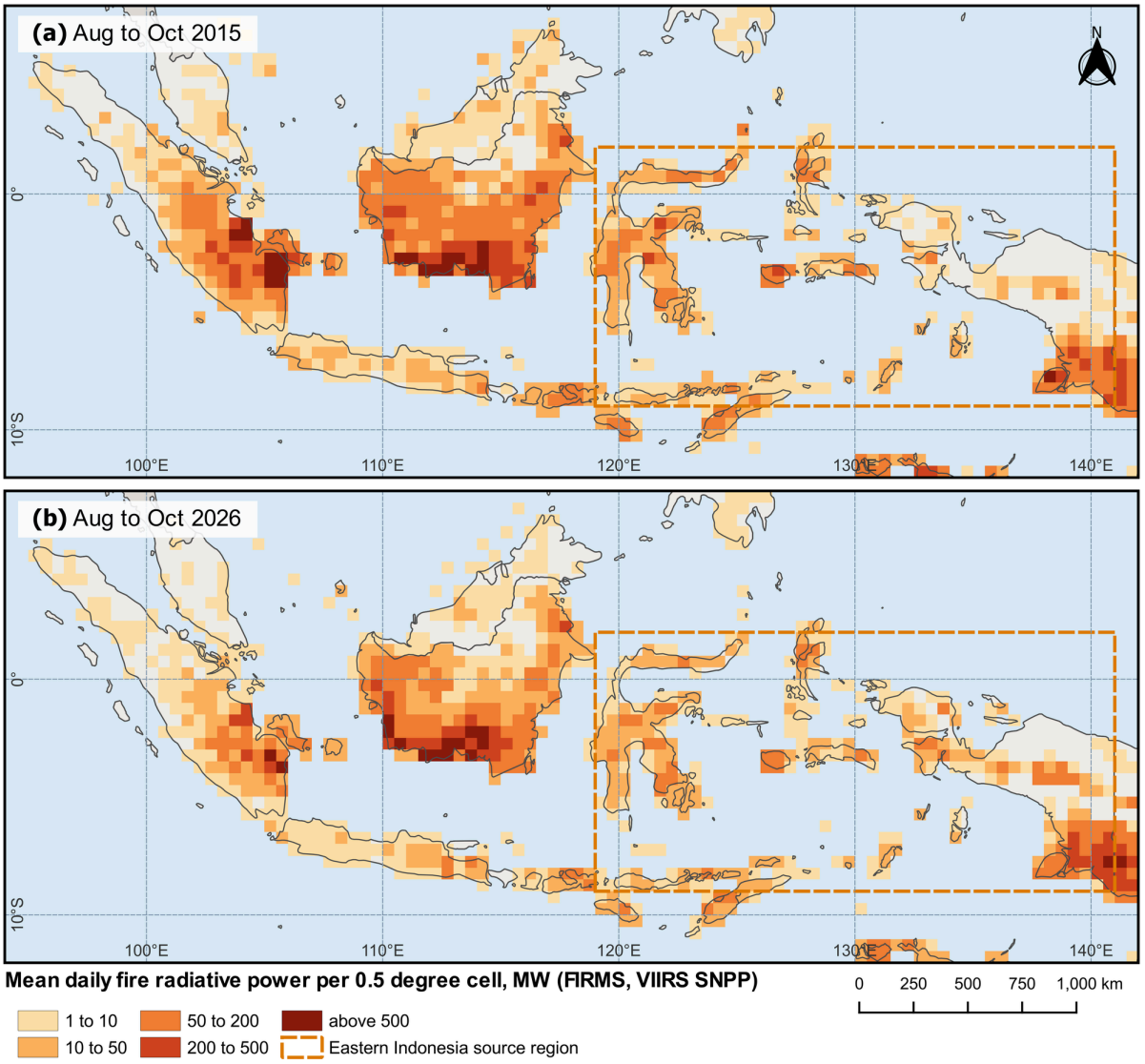


Figure 7. *Mean daily fire radiative power per 0.5° cell, August to October (FIRMS, VIIRS SNPP): (a) 2015; (b) 2026. The dashed box marks the eastern Indonesia source region. All detected fires are shown; the regional totals in Table 2 use Indonesian land cells only.*

Winds and rain favoured the corridor in 2026. The mean northward wind at 850 hPa over the gateway was the third strongest of 15 seasons (1.46 m s^{-1}) and strongest in August (2.03 m s^{-1}), and the corridor had the second-lowest rainfall (7.8 mm per day); both checks passed (Fig. 8c, d). But 2015 was first on both measures (1.73 m s^{-1} and 7.2 mm per day), so neither transport nor rain distinguishes 2026 from 2015. GFAS placed 2026 far above every earlier season (5.0 against 3.7 Tg of organic plus black carbon over Indonesia), but its FRP doubled from 2015 to 2026 while FIRMS FRP fell by 29%, which points to the version change in January 2026; GFAS is therefore not used for the comparison.

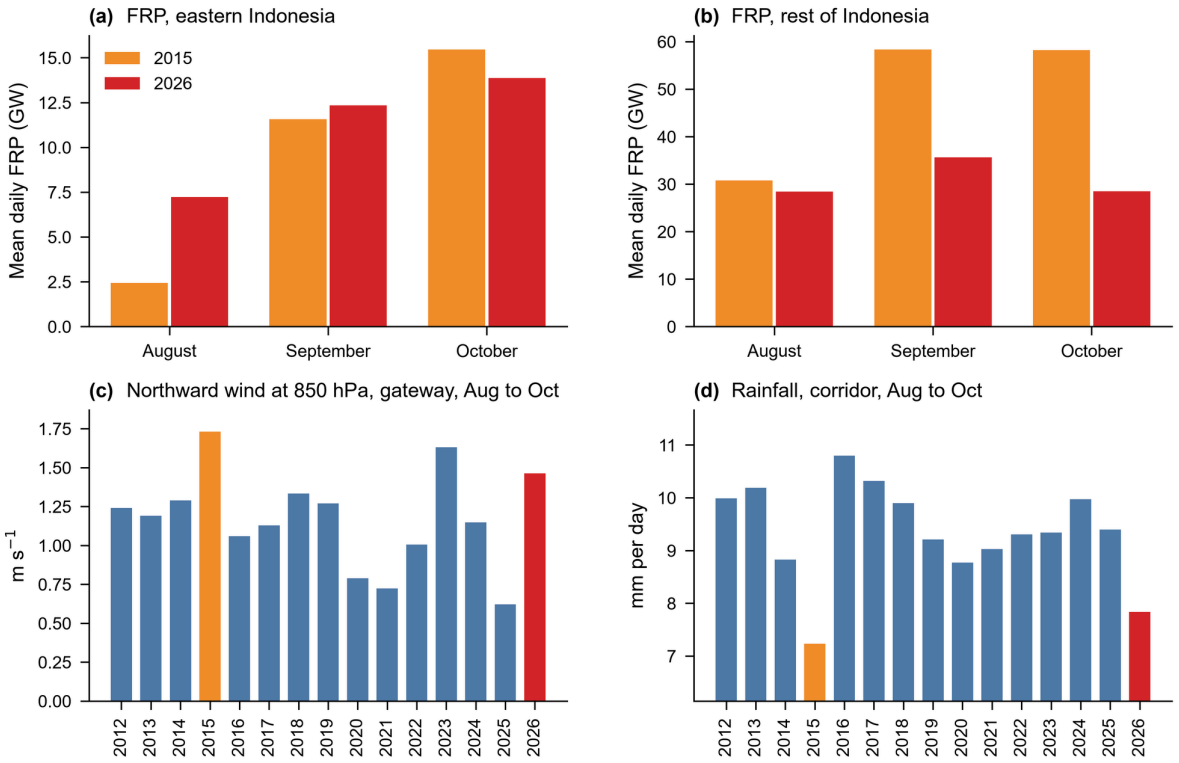


Figure 8. *Drivers: mean daily FRP by month (FIRMS, VIIRS SNPP) in (a) eastern Indonesia and (b) the rest of Indonesia, 2015 and 2026; (c) mean northward wind at 850 hPa over the gateway band and (d) mean corridor rainfall, August to October, 2012 to 2026 (ERA5); 2026 in red, 2015 in orange.*

4.5 Ground-based confirmation

VIIRS agreed well with AERONET at Koronadal (r = 0.81, 331 matched days), Sorong (0.96) and Makassar (0.91), with VIIRS higher by 0.02 to 0.05; agreement at Manila, an urban site poorly represented by a 1° cell, was weaker (0.44). AERONET and VIIRS both placed 2026 above 2015 at Sorong (AERONET 0.68 against 0.14), Makassar (0.38 against 0.21) and, by a very small margin, Manila, so both checks of Test 6 passed. At Koronadal, the site nearest the corridor, AERONET placed 2026 above 2015, and 2026 was its highest of 11 seasons, but VIIRS on the same days gave the opposite order (Supplementary Section S3; Fig. S3). Manila showed nothing unusual in 2026 (seventh of nine seasons), consistent with smoke reaching the corridor from the south-east rather than across Luzon.

4.6 MERRA-2 and the satellites

MERRA-2 AOD sampled on VIIRS cell-days was about half the VIIRS value in the corridor (0.07 to 0.15 against 0.12 to 0.20 for August to September), and lower on retrieval days than on all days in every season (by 0.016 on average), confirming that the satellites see the corridor mainly on its cleaner days. MERRA-2 ranked 2026, 2015 and 2019 in the same order as VIIRS but disagreed on the quieter seasons, and the ranking check failed (Spearman 0.65 for August to September; a provisional 0.39 for August to October, 2012 to 2025, pending MERRA-2 for October 2026; Fig. S4). Over 1980 to 2026, MERRA-2 total AOD is led by the volcanic years 1991 and 1982, and its smoke shows a step between eras: the 1980 to 2002 mean over Kalimantan is 3.7

times that of 2003 to 2025, consistent with the change from monthly fire inventories before 2010 to daily QFED emissions (Darmenov and da Silva 2015). In MERRA-2 smoke, 2026 ties with 1997 in the corridor (1.94 against 1.90 μg m^{-3}) and is well below 1997 in eastern Indonesia, so a record since 1980 cannot be claimed.

5. Discussion

5.1 An eastern, early season

The 2026 record in the typhoon zone was not a record of burning. Indonesia as a whole burned less than in 2015, and conditions for transport and against removal, though favourable, were no more so than in 2015. What differed was the geography and timing of the fires. Eastern Indonesia, the source nearest the corridor, burned more than in any season since 2012, and did so from August, when the northward flow over the gateway was strongest. Smoke from Sulawesi, Maluku and northern Papua has a short path to the corridor, whereas smoke from Sumatra and Kalimantan must travel 1,500 km or more, with more opportunity to be rained out. This agrees with the transport climatology of Xian et al. (2013), in which pathways follow the low-level flow; it also suggests that southern Papua, which that study found to export smoke westward in boreal summer, contributed less to the corridor than its share of the burning would imply. The early start matters too: August and September smoke meets the corridor in the core of the typhoon season, whereas the 2015 peak came in October.

Two limits apply. FRP measures flaming intensity seen from orbit and understates smouldering peat fires, which were extensive in Sumatra and Kalimantan in 2015 (Huijnen et al. 2016); the 2015 advantage in total emissions is therefore probably larger than the FRP ratio suggests, which strengthens rather than weakens the conclusion that the corridor record did not come from total burning. And monthly winds hide the day-to-day events, such as typhoon-driven streamers, that carry smoke in pulses.

5.2 Typhoons: visible streamers, no robust export signal

The conceptual picture in which typhoon inflow draws Maritime Continent smoke into the monsoon flow (Reid et al. 2012, 2016b) is well supported by observations of individual events, and the Choi-wan streamer of 2026 is another example; aircraft and ship observations in 2019 showed similar transport into the tropical northwest Pacific (Hilario et al. 2021; Reid et al. 2023). The question here was narrower: whether typhoon days, taken together, carry more smoke into the open Pacific than other days of the same seasons. They did not do so robustly. The apparent effect was explained as well by the timing of typhoons within smoky seasons as by the storms themselves, and the pattern that seemed to describe how a typhoon entry produces a pulse of export failed on independent years. Several processes can cancel in aggregate: the storms that accelerate the flow also rain on the smoke and, after they pass, can weaken or reverse the flow (Reid et al. 2016b). The result does not show that typhoons have no effect; it shows that the effect, if present, is not large or consistent enough to stand out from chance in 47 seasons of reanalysis.

Two caveats bound this conclusion. MERRA-2 is the only multi-decadal source of daily smoke fluxes used here, and its fire emissions are monthly before 2010, so day-to-day variability in the earlier seasons comes from transport alone. And satellite AOD cannot test the effect directly, because typhoon days are cloudy. A test across several aerosol reanalyses, such as the CAMS and NAAPS reanalyses (Lynch et al. 2016; Inness et al. 2019),

would be the natural next step. The view that the active 2026 typhoon season worsened the regional haze is not examined directly here, but the absence of a robust export signal argues for caution in attributing haze to typhoons.

5.3 What a reanalysis can and cannot show

The comparison with VIIRS shows what MERRA-2 can support. It identified the largest smoke seasons but at half the satellite AOD, and it did not rank the quieter seasons reliably; across eras its smoke reflects changes in fire inventories, and its total AOD reflects volcanic aerosol. A record in a reanalysis should therefore be confirmed with observations before it is claimed, as here, and long-term comparisons in MERRA-2 should be restricted to periods with consistent emissions. The factor-of-two difference in AOD also cautions against reading reanalysis smoke concentrations as absolute values in this region, which is among the most difficult for aerosol reanalyses (Xian et al. 2024).

5.4 Limitations

The record rests on two VIIRS instruments using one retrieval algorithm, cross-checked with MODIS and with four ground sites, none inside the corridor. Satellite AOD samples clear days, and AOD includes sea salt, although the smoke indicators point the same way. VIIRS data for 30 and 31 October 2026 were not yet processed; MERRA-2 for October 2026 and standard FIRMS data for 2026 were not yet released. The affected checks (O2, Test 2 with October 2026, and the FIRMS archive step) will be rerun unchanged and reported. The driver analysis is descriptive and uses monthly means, and peat emissions are poorly represented by FRP.

6. Conclusion

Typhoon days did not robustly increase smoke export into the western North Pacific typhoon zone over 24 seasons, and the pattern suggested by the exploratory analysis did not replicate in 23 independent seasons; streamers such as the one drawn towards Super Typhoon Choi-wan in 2026 are real, but they do not add up to a robust signal. Judged by independent satellite observations, August to October 2026 was nevertheless the strongest smoke season of the VIIRS era in that zone: narrowly above 2015 over the full season, and well above it in August and September. The record came from early and intense burning in eastern Indonesia, close to the zone, rather than from more burning overall, which was greater in 2015, or from unusually favourable winds or rain. Fixing the criteria before computation, testing against placebos and replicating on unseen years turned a suggestive exploratory analysis into a smaller set of claims that hold, and set aside two that did not.

Acknowledgements

Imagery in Fig. 3a and b is from the NASA Worldview application (https://worldview.earthdata.nasa.gov), part of the NASA Earth Science Data and Information System (ESDIS). The author thanks the principal investigators and site managers of the AERONET sites used here (ND Marbel University in Koronadal, Manila Observatory, Sorong and Makassar) for establishing and maintaining them, and NASA, NOAA and ECMWF for the open data. ERA5 and GFAS data contain modified Copernicus Climate Change Service and Copernicus

Atmosphere Monitoring Service information (2026); neither the European Commission nor ECMWF is responsible for any use of this information.

Statements and Declarations

Funding

The author declares that no funds, grants or other support were received during the preparation of this manuscript.

Competing interests

The author has no relevant financial or non-financial interests to disclose.

Data availability

All data used are openly available (Table S1). The notebooks, the dated test criteria and results, and the derived data are available at Zenodo (Tai 2026; https://doi.org/10.5281/zenodo.24054200).

Ethics approval

Not applicable. This study used only openly available secondary data and involved no human participants or animals.

References

Buchard V, Randles CA, da Silva AM, et al. (2017) The MERRA-2 aerosol reanalysis, 1980 onward. Part II: evaluation and case studies. J Clim 30:6851–6872. https://doi.org/10.1175/JCLI-D-16-0613.1

Camargo SJ, Sobel AH (2005) Western North Pacific tropical cyclone intensity and ENSO. J Clim 18:2996–3006. https://doi.org/10.1175/JCLI3457.1

Chan JCL (1985) Tropical cyclone activity in the northwest Pacific in relation to the El Niño/Southern Oscillation phenomenon. Mon Weather Rev 113:599–606. https://doi.org/10.1175/1520-0493(1985)113<0599:TCAITN>2.0.CO;2

Crippa P, Castruccio S, Archer-Nicholls S, et al. (2016) Population exposure to hazardous air quality due to the 2015 fires in Equatorial Asia. Sci Rep 6:37074. https://doi.org/10.1038/srep37074

Darmenov A, da Silva A (2015) The Quick Fire Emissions Dataset (QFED): documentation of versions 2.1, 2.2 and 2.4. NASA Technical Report Series on Global Modeling and Data Assimilation, NASA/TM-2015-104606, Vol. 38

Daily Tribune (2026) Indonesian haze affects Calabarzon, Mimaropa. Daily Tribune, 2 September 2026. https://tribune.net.ph/2026/09/01/indonesian-haze-affects-calabarzon-mimaropa

Echeminada P (2026) Haze from Indonesian fire continue to pollute air in NorMin. Daily Tribune, 21 September 2026. https://tribune.net.ph/2026/09/21/haze-from-indonesian-fire-continue-to-pollute-air-in-normin

Eck TF, Holben BN, Reid JS, Dubovik O, Smirnov A, O'Neill NT, Slutsker I, Kinne S (1999) Wavelength dependence of the optical depth of biomass burning, urban, and desert dust aerosols. J Geophys Res 104:31333–31349. https://doi.org/10.1029/1999JD900923

Efron B, Tibshirani RJ (1993) An introduction to the bootstrap. Chapman and Hall, New York

Fanin T, van der Werf GR (2017) Precipitation–fire linkages in Indonesia (1997–2015). Biogeosciences 14:3995–4008. https://doi.org/10.5194/bg-14-3995-2017

Field RD, van der Werf GR, Fanin T, Fetzer EJ, Fuller R, Jethva H, Levy R, Livesey NJ, Luo M, Torres O, Worden HM (2016) Indonesian fire activity and smoke pollution in 2015 show persistent nonlinear sensitivity to El Niño-induced drought. Proc Natl Acad Sci USA 113:9204–9209. https://doi.org/10.1073/pnas.1524888113

Field RD, van der Werf GR, Shen SSP (2009) Human amplification of drought-induced biomass burning in Indonesia since 1960. Nat Geosci 2:185–188. https://doi.org/10.1038/ngeo443

Gelaro R, McCarty W, Suárez MJ, et al. (2017) The Modern-Era Retrospective Analysis for Research and Applications, Version 2 (MERRA-2). J Clim 30:5419–5454. https://doi.org/10.1175/JCLI-D-16-0758.1

Giles DM, Sinyuk A, Sorokin MG, et al. (2019) Advancements in the Aerosol Robotic Network (AERONET) Version 3 database – automated near-real-time quality control algorithm with improved cloud screening for Sun photometer aerosol optical depth (AOD) measurements. Atmos Meas Tech 12:169–209. https://doi.org/10.5194/amt-12-169-2019

Hersbach H, Bell B, Berrisford P, et al. (2020) The ERA5 global reanalysis. Q J R Meteorol Soc 146:1999–2049. https://doi.org/10.1002/qj.3803

Hilario MRA, Crosbie E, Shook M, et al. (2021) Measurement report: Long-range transport patterns into the tropical northwest Pacific during the CAMP2Ex aircraft campaign: chemical composition, size distributions, and the impact of convection. Atmos Chem Phys 21:3777–3802. https://doi.org/10.5194/acp-21-3777-2021

Holben BN, Eck TF, Slutsker I, et al. (1998) AERONET – a federated instrument network and data archive for aerosol characterization. Remote Sens Environ 66:1–16. https://doi.org/10.1016/S0034-4257(98)00031-5

Hsu NC, Lee J, Sayer AM, Kim W, Bettenhausen C, Tsay SC (2019) VIIRS Deep Blue aerosol products over land: extending the EOS long-term aerosol data records. J Geophys Res Atmos 124:4026–4053. https://doi.org/10.1029/2018JD029688

Huijnen V, Wooster MJ, Kaiser JW, et al. (2016) Fire carbon emissions over maritime southeast Asia in 2015 largest since 1997. Sci Rep 6:26886. https://doi.org/10.1038/srep26886

Inness A, Ades M, Agustí-Panareda A, et al. (2019) The CAMS reanalysis of atmospheric composition. Atmos Chem Phys 19:3515–3556. https://doi.org/10.5194/acp-19-3515-2019

Inquirer (2026) Indonesian fires bring haze to the Philippines. Philippine Daily Inquirer/Asia News Network, 15 October 2026. https://www.thestar.com.my/aseanplus/aseanplus-news/2026/10/15/indonesian-fires-bring-haze-to-the-philippines

Kaiser JW, Heil A, Andreae MO, et al. (2012) Biomass burning emissions estimated with a global fire assimilation system based on observed fire radiative power. Biogeosciences 9:527–554. https://doi.org/10.5194/bg-9-527-2012

Knapp KR, Kruk MC, Levinson DH, Diamond HJ, Neumann CJ (2010) The International Best Track Archive for Climate Stewardship (IBTrACS): unifying tropical cyclone data. Bull Am Meteorol Soc 91:363–376. https://doi.org/10.1175/2009BAMS2755.1

Koplitz SN, Mickley LJ, Marlier ME, et al. (2016) Public health impacts of the severe haze in Equatorial Asia in September–October 2015: demonstration of a new framework for informing fire management strategies to reduce downwind smoke exposure. Environ Res Lett 11:094023. https://doi.org/10.1088/1748-9326/11/9/094023

Levy RC, Mattoo S, Munchak LA, Remer LA, Sayer AM, Patadia F, Hsu NC (2013) The Collection 6 MODIS aerosol products over land and ocean. Atmos Meas Tech 6:2989–3034. https://doi.org/10.5194/amt-6-2989-2013

Lynch P, Reid JS, Westphal DL, et al. (2016) An 11-year global gridded aerosol optical thickness reanalysis (v1.0) for atmospheric and climate sciences. Geosci Model Dev 9:1489–1522. https://doi.org/10.5194/gmd-9-1489-2016

Madden RA, Julian PR (1971) Detection of a 40–50 day oscillation in the zonal wind in the tropical Pacific. J Atmos Sci 28:702–708. https://doi.org/10.1175/1520-0469(1971)028<0702:DOADOI>2.0.CO;2

Maloney ED, Hartmann DL (2001) The Madden–Julian oscillation, barotropic dynamics, and North Pacific tropical cyclone formation. Part I: observations. J Atmos Sci 58:2545–2558. https://doi.org/10.1175/1520-0469(2001)058<2545:TMJOBD>2.0.CO;2

Marlier ME, DeFries RS, Voulgarakis A, Kinney PL, Randerson JT, Shindell DT, Chen Y, Faluvegi G (2013) El Niño and health risks from landscape fire emissions in southeast Asia. Nat Clim Change 3:131–136. https://doi.org/10.1038/nclimate1658

Nosek BA, Ebersole CR, DeHaven AC, Mellor DT (2018) The preregistration revolution. Proc Natl Acad Sci USA 115:2600–2606. https://doi.org/10.1073/pnas.1708274114

Page SE, Siegert F, Rieley JO, Boehm HDV, Jaya A, Limin S (2002) The amount of carbon released from peat and forest fires in Indonesia during 1997. Nature 420:61–65. https://doi.org/10.1038/nature01131

Randles CA, da Silva AM, Buchard V, et al. (2017) The MERRA-2 aerosol reanalysis, 1980 onward. Part I: system description and data assimilation evaluation. J Clim 30:6823–6850. https://doi.org/10.1175/JCLI-D-16-0609.1

Reid JS, Xian P, Hyer EJ, et al. (2012) Multi-scale meteorological conceptual analysis of observed active fire hotspot activity and smoke optical depth in the Maritime Continent. Atmos Chem Phys 12:2117–2147. https://doi.org/10.5194/acp-12-2117-2012

Reid JS, Hyer EJ, Johnson RS, et al. (2013) Observing and understanding the Southeast Asian aerosol system by remote sensing: an initial review and analysis for the Seven Southeast Asian Studies (7SEAS) program. Atmos Res 122:403–468. https://doi.org/10.1016/j.atmosres.2012.06.005

Reid JS, Lagrosas ND, Jonsson HH, et al. (2015) Observations of the temporal variability in aerosol properties and their relationships to meteorology in the summer monsoonal South China Sea/East Sea: the scale-dependent role of monsoonal flows, the Madden–Julian Oscillation, tropical cyclones, squall lines and cold pools. Atmos Chem Phys 15:1745–1768. https://doi.org/10.5194/acp-15-1745-2015

Reid JS, Xian P, Holben BN, et al. (2016a) Aerosol meteorology of the Maritime Continent for the 2012 7SEAS southwest monsoon intensive study – Part 1: regional-scale phenomena. Atmos Chem Phys 16:14041–14056. https://doi.org/10.5194/acp-16-14041-2016

Reid JS, Lagrosas ND, Jonsson HH, et al. (2016b) Aerosol meteorology of Maritime Continent for the 2012 7SEAS southwest monsoon intensive study – Part 2: Philippine receptor observations of fine-scale aerosol behavior. Atmos Chem Phys 16:14057–14078. https://doi.org/10.5194/acp-16-14057-2016

Reid JS, Maring HB, Narisma GT, et al. (2023) The coupling between tropical meteorology, aerosol lifecycle, convection, and radiation during the Cloud, Aerosol and Monsoon Processes Philippines Experiment (CAMP2Ex). Bull Am Meteorol Soc 104:E1179–E1205. https://doi.org/10.1175/BAMS-D-21-0285.1

Sayer AM, Hsu NC, Lee J, Bettenhausen C, Kim WV, Smirnov A (2018) Satellite Ocean Aerosol Retrieval (SOAR) algorithm extension to S-NPP VIIRS as part of the "Deep Blue" aerosol project. J Geophys Res Atmos 123:380–400. https://doi.org/10.1002/2017JD027412

Sayer AM, Hsu NC, Lee J, Kim WV, Dutcher ST (2019) Validation, stability, and consistency of MODIS Collection 6.1 and VIIRS Version 1 Deep Blue aerosol data over land. J Geophys Res Atmos 124:4658–4688. https://doi.org/10.1029/2018JD029598

Schroeder W, Oliva P, Giglio L, Csiszar IA (2014) The New VIIRS 375 m active fire detection data product: algorithm description and initial assessment. Remote Sens Environ 143:85–96. https://doi.org/10.1016/j.rse.2013.12.008

Shetty D (2026) Indonesian wildfires cause air pollution levels to rise to hazardous levels in Southeast Asia. Health Policy Watch, 4 September 2026. https://healthpolicy-watch.news/indonesian-wildfires-cause-air-pollution-levels-to-rise-to-hazardous-levels-in-southeast-asia/

The Straits Times (2026) Haze caused by many factors, but repeat of 2015 crisis unlikely due to later onset of El Nino: Singapore experts. The Straits Times/Asia News Network, 3 September 2026. https://www.thestar.com.my/aseanplus/aseanplus-news/2026/09/03/haze-caused-by-many-factors-but-repeat-of-2015-crisis-unlikely-due-to-later-onset-of-el-nino-singapore-experts

Tai LR (2026) Do typhoons pull Indonesian smoke into the Pacific? Code, pre-registered test criteria and results [Data set]. Zenodo. https://doi.org/10.5281/zenodo.24054200

van der Werf GR, Randerson JT, Giglio L, et al. (2017) Global fire emissions estimates during 1997–2016. Earth Syst Sci Data 9:697–720. https://doi.org/10.5194/essd-9-697-2017

Wang B, Chan JCL (2002) How strong ENSO events affect tropical storm activity over the western North Pacific. J Clim 15:1643–1658. https://doi.org/10.1175/1520-0442(2002)015<1643:HSEEAT>2.0.CO;2

Wang J, Ge C, Yang Z, et al. (2013) Mesoscale modeling of smoke transport over the Southeast Asian Maritime Continent: interplay of sea breeze, trade wind, typhoon, and topography. Atmos Res 122:486–503. https://doi.org/10.1016/j.atmosres.2012.05.009

Wheeler MC, Hendon HH (2004) An all-season real-time multivariate MJO index: development of an index for monitoring and prediction. Mon Weather Rev 132:1917–1932. https://doi.org/10.1175/1520-0493(2004)132<1917:AARMMI>2.0.CO;2

Wilks DS (2016) “The stippling shows statistically significant grid points”: how research results are routinely overstated and overinterpreted, and what to do about it. Bull Am Meteorol Soc 97:2263–2273. https://doi.org/10.1175/BAMS-D-15-00267.1

Wooster MJ, Roberts G, Perry GLW, Kaufman YJ (2005) Retrieval of biomass combustion rates and totals from fire radiative power observations: FRP derivation and calibration relationships between biomass consumption and fire radiative energy release. J Geophys Res 110:D24311. https://doi.org/10.1029/2005JD006318

Xian P, Reid JS, Atwood SA, Johnson RS, Hyer EJ, Westphal DL, Sessions W (2013) Smoke aerosol transport patterns over the Maritime Continent. Atmos Res 122:469–485. https://doi.org/10.1016/j.atmosres.2012.05.006

Xian P, Reid JS, Ades M, et al. (2024) Intercomparison of aerosol optical depths from four reanalyses and their multi-reanalysis consensus. Atmos Chem Phys 24:6385–6411. https://doi.org/10.5194/acp-24-6385-2024

Supplementary Information

Do typhoons pull Indonesian smoke into the Pacific? A pre-registered test, and the record 2026 season

---

Contents: Table S1, open data; Section S1, test criteria and amendments; Section S2, data versions and checks; Section S3, ground stations; Section S4, supplementary figures (Figs. S1 to S4). Analyses are in notebooks 01 to 19, with the dated criteria and results of every test, openly available at Zenodo (https://doi.org/10.5281/zenodo.24054200).

Open data

Table S1. *Open data used in the study. All are free; NASA Earthdata, Copernicus and FIRMS require a free account or key.*

Dataset	Version or date	Resolution	Use	Reference
VIIRS Deep Blue, SNPP (AERDB_D3_VIIRS_SNPP)	Version 2; 2012 to 2026	1°, daily	AOD, Ångström exponent, fine-mode fraction	Hsu et al. (2019)
VIIRS Deep Blue, NOAA-20 (AERDB_D3_VIIRS_NOAA20)	Version 2; 2018 to 2026	1°, daily	Second instrument	Hsu et al. (2019)
MODIS Aqua (MYD08_D3)	Collection 6.1; 2002 to 2026	1°, daily	Record back to 2002	Levy et al. (2013)
MERRA-2 (M2T1NXAER)	1980 to 2026	0.5° × 0.625°, daily means	Smoke fluxes; AOD comparison	Gelaro et al. (2017); Randles et al. (2017)
GEOS-FP (tavg3_2d_aer_Nx)	28 September to 7 October 2026	0.25° × 0.3125°, 3-hourly	Choi-wan case	NASA GMAO
NASA Worldview snapshots	6 October 2026; VIIRS Deep Blue version 2.1	About 1 km, image	Choi-wan case (Fig. 3a, b)	NASA ESDIS
FIRMS VIIRS active fires (SNPP, NOAA-20)	Standard processing 2012 to 2025; near-real-time 2026	375 m, summed to 0.5° daily	Fire radiative power	Schroeder et al. (2014)
CAMS GFAS	v1.2 to 2025; v1.4.2 from 2026	0.1°, daily	Fire emissions (secondary)	Kaiser et al. (2012)
ERA5 monthly means	2012 to 2026	0.25°, monthly	Winds at 850 and 700 hPa; rainfall	Hersbach et al. (2020)
ERA5 daily statistics and hourly fields	August to October 2026	0.25°, daily and hourly	Case study; trajectories	Hersbach et al. (2020)
AERONET	Version 3, Levels 1.5 and 2.0	Site, daily	Ground check	Giles et al. (2019)

IBTrACS	v04r01; 1980 to 2026	Track points, 3-hourly	Typhoon days and tracks	Knapp et al. (2010)
RMM index (Bureau of Meteorology)	To February 2024	Daily	MJO control	Wheeler and Hendon (2004)
Oceanic Niño Index (NOAA CPC)	1950 to 2026	Three-month seasons	ENSO state	NOAA Climate Prediction Center
Natural Earth	Admin 0 countries, 1:50 million	Vector	Country masks; maps	naturalearthdata.com

Section S1. Test criteria and amendments

Each test's criteria were agreed and dated before computation. Amendments made after agreement are listed here with their timing; none changed a pass level after results were seen.

Test 2 (1 November 2026). Clarification before computation: the calendar-day baseline removes the mean seasonal cycle and each season's own mean. Data note after the run: the RMM index ends on 24 February 2024, so the MJO control (C4) covers 2003 to 2023. The leave-one-season-out and variant results are shown in Fig. S1.

Test 2b (1 November 2026). No amendments. The pre-registered pulse window (days 0 and +1) missed a surge at days −2 and −1 in 1980 to 2002; this was observed after the fact and was not used to rescue the test.

Test 3 (2 November 2026). Before computation: the fine-mode fraction over the ocean was added as a reported indicator; VIIRS version 2 was fixed for every season, including 2026 (Section S2). Data note: SNPP has 52 of 61 days in August to September 2022; missing days count as days without retrievals.

Test 3c (3 November 2026). Data note before computation: VIIRS 30 and 31 October 2026 were not yet processed and count as days without retrievals; if released, Test 3c will be rerun unchanged and both results reported.

Test 3d (6 November 2026). No amendments.

Test 4 (6 November 2026). Before computation: the Indonesian mask uses the land in each 0.5° cell (5 × 5 sample points) instead of the cell centre, because the centre rule drops coastal cells, where many peat fires lie.

Test 6 (6 November 2026). Before the numbers were printed, the rule G2 was written out: a site counts for 2026 if AERONET's 2026 mean exceeds its 2015 mean and VIIRS on that site's matched days does too.

Section S2. Data versions and checks

VIIRS Deep Blue. Version 2 is served for 2012 to 2025 and version 2.1 from mid-June 2026. On 60 days with both versions (12 June to 29 October 2026), corridor AOD in version 2.1 differs from version 2 by −1.5% (SNPP) and −1.2% (NOAA-20), with daily r = 1.000; the Ångström exponent and fine-mode fraction differ by up to 9% (NOAA-20). Version 2 was used for every season.

FIRMS. Days with no detection anywhere in the download area (94 to 160° E, 12° S to 8° N) are satellite outages and were treated as missing: SNPP 1 to 10 August 2022, 26 September 2024 and 3 August 2026; NOAA-20 30 September 2023. Standard processing ended on 31 July 2026 when the data were downloaded, so 2026 is near-real-time data.

GFAS. Version 1.2 (MODIS) runs to 31 December 2025 and version 1.4.2 (VIIRS, with MODIS while available) from 1 January 2026, without overlap. GFAS labels each daily mean with the following day; dates were shifted back by one day.

MODIS Aqua. Corridor coverage is 26 to 38% of cell-days per season (VIIRS 35 to 53%), so several seasons fall below the 30% rule. Over August to September, 2005 had the highest MODIS value of all seasons (0.181) but only 26% coverage; over August to October it passed the rule and ranked sixth (Fig. S2).

MERRA-2. Fire emissions are RETROv2 (1980 to 1996) and GFED3.1 (1997 to 2009), both monthly, then daily QFED from 2010. Comparisons across these eras are unreliable.

Section S3. Ground stations

AERONET version 3 Level 1.5 daily means, August to October, AOD converted to 550 nm (Fig. S3). Koronadal (ND Marbel University; 124.8° E, 6.5° N): 331 matched days, r = 0.81, bias (VIIRS minus AERONET) +0.05; AERONET 2015 0.31, 2026 0.34 (first of 11 seasons); VIIRS on matched days 0.41 and 0.32.

Manila Observatory (121.1° E, 14.6° N): 194 matched days, r = 0.44, bias −0.06; AERONET 2015 0.265, 2026 0.274 (seventh of nine); VIIRS 0.2079 and 0.2084.

Sorong (131.3° E, 0.9° S): 234 matched days, r = 0.96, bias +0.02; AERONET 2015 0.14, 2026 0.68 (first of six); VIIRS 0.17 and 0.62.

Makassar (119.6° E, 5.0° S): 512 matched days, r = 0.91, bias +0.03; AERONET 2015 0.21, 2026 0.38 (first of eight); VIIRS 0.25 and 0.36.

No AERONET site inside the corridor (Guam, Tinian, Apra Harbor, Manus) has data for August to October in these seasons.

Section S4. Supplementary figures

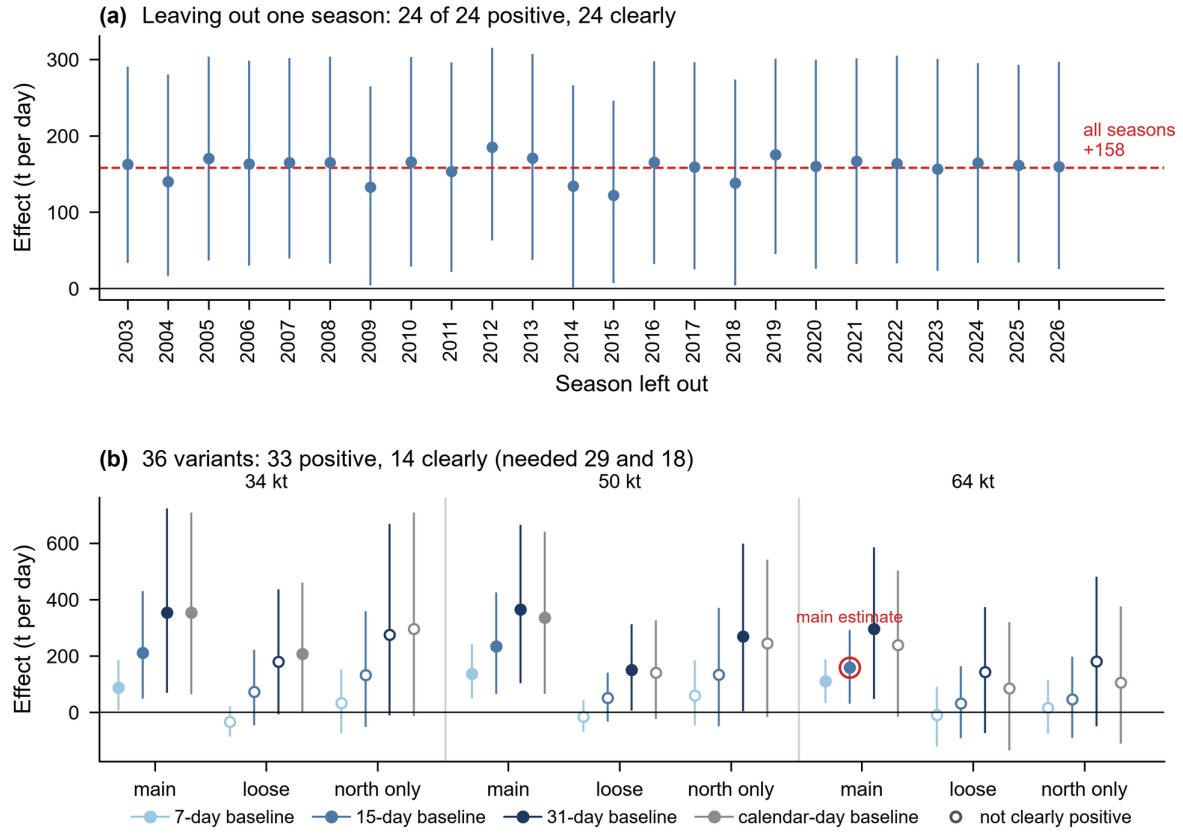


Figure S1. *Robustness of the typhoon-day effect on smoke inflow to the corridor (Test 2; MERRA-2, 2003 to 2026): (a) the effect with each season left out in turn (C3); (b) the 36 variants of intensity threshold (34, 50 and 64 kt), typhoon box (main, loose, north only) and baseline (C2). Bars: 95% intervals from resampling seasons; filled markers: clearly positive; circled: the main estimate (64 kt, main box, 15-day baseline; +158 t per day).*

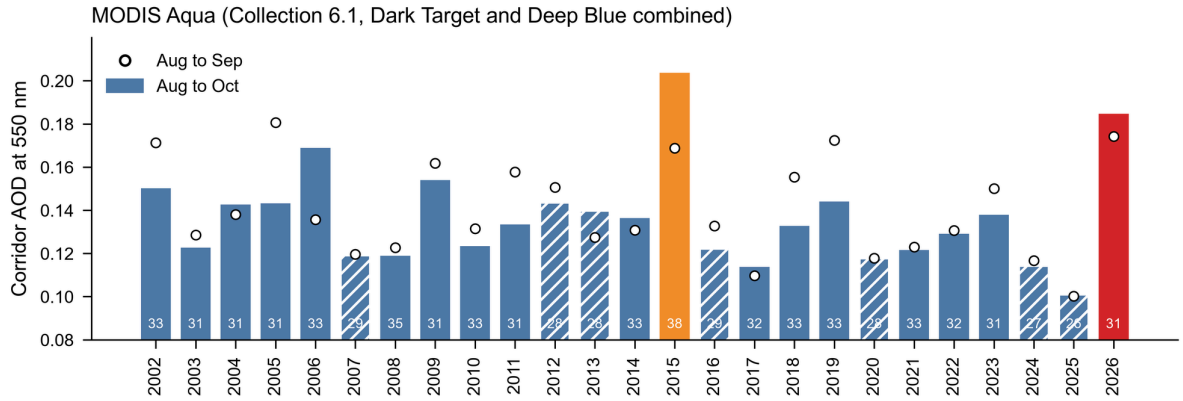


Figure S2. *Mean corridor AOD at 550 nm from MODIS Aqua (Collection 6.1, Dark Target and Deep Blue combined), August to October (bars) and August to September (dots), 2002 to 2026. Numbers in the bars give the percentage of corridor cell-days with a retrieval, August to October; hatched bars fall below the 30% coverage rule (O0); 2026 in red, 2015 in orange.*

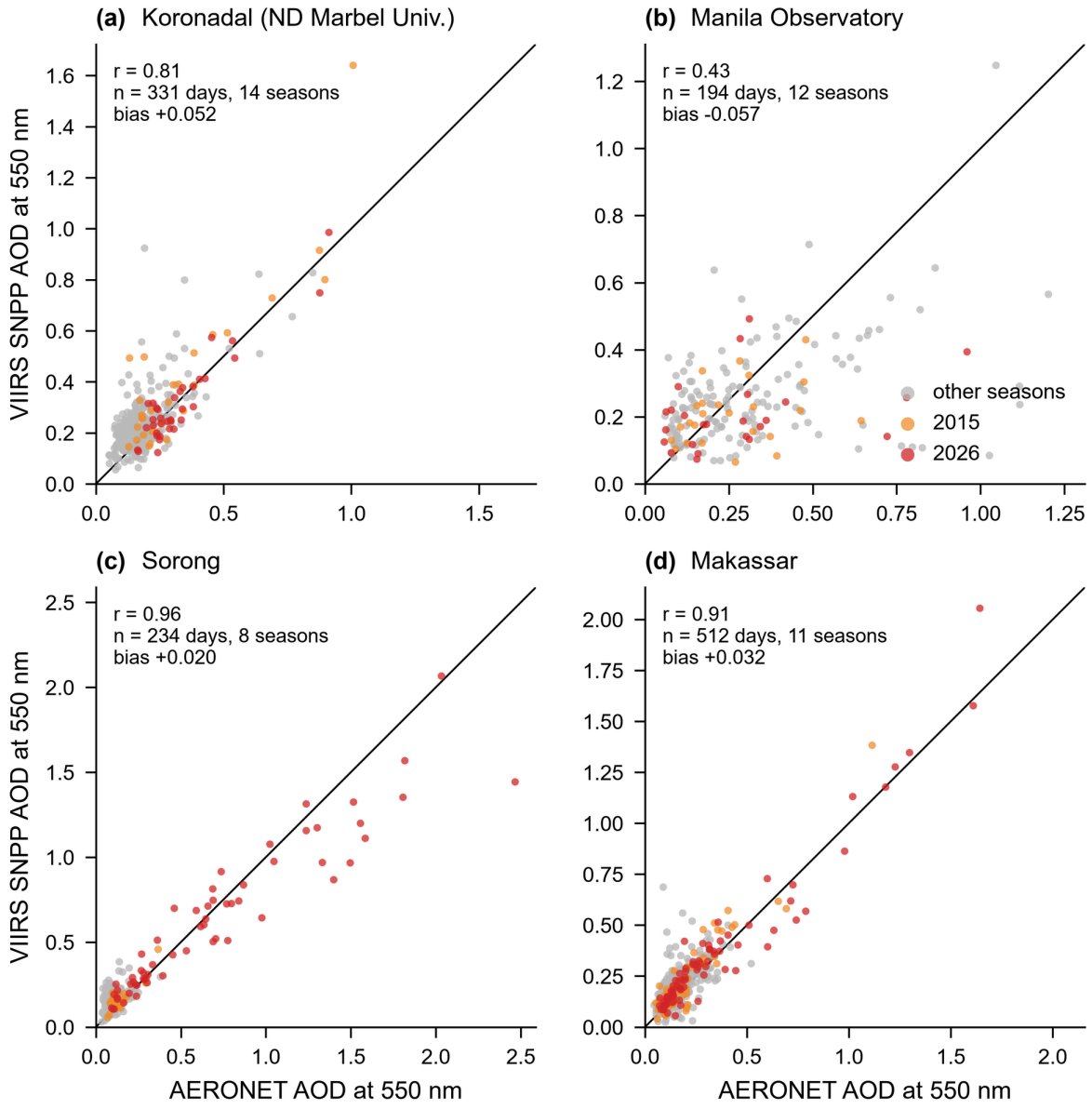


Figure S3. *Daily AOD at 550 nm from VIIRS SNPP (nearest 1° cell) against AERONET Level 1.5, August to October of all seasons with both: (a) Koronadal, (b) Manila Observatory, (c) Sorong, (d) Makassar. 2026 in red, 2015 in orange; the line is 1:1; bias is VIIRS minus AERONET.*

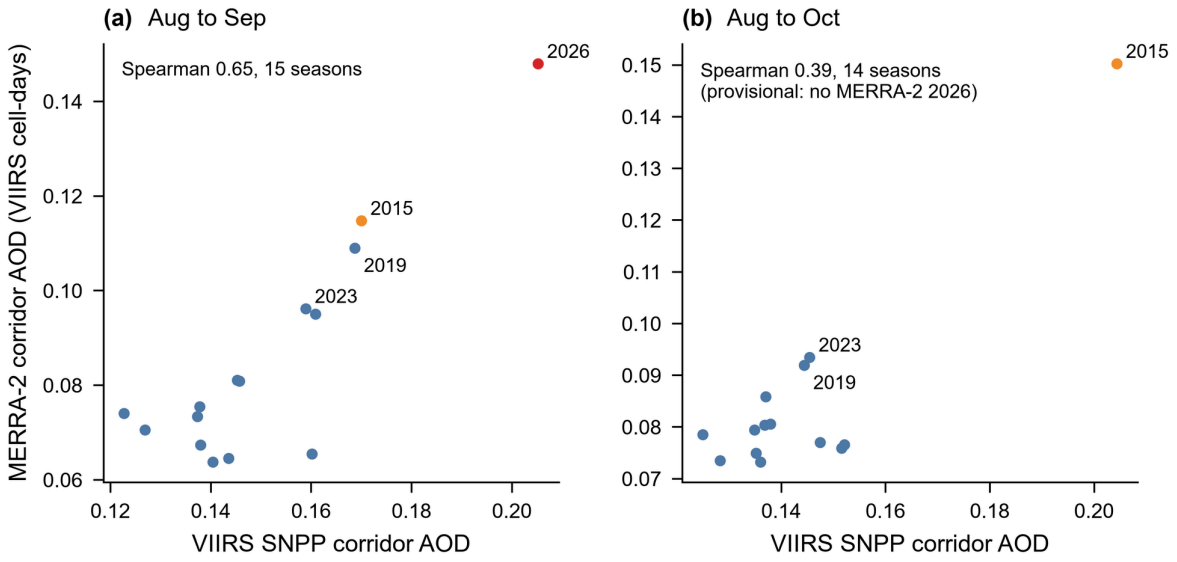


Figure S4. *Season-mean corridor AOD from MERRA-2, sampled on the cell-days with VIIRS retrievals, against VIIRS SNPP (check O2): (a) August to September, 2012 to 2026; (b) August to October, 2012 to 2025, as MERRA-2 for October 2026 is not yet released. 2026 in red, 2015 in orange.*

References

Gelaro R, McCarty W, Suárez MJ, et al. (2017) The Modern-Era Retrospective Analysis for Research and Applications, Version 2 (MERRA-2). J Clim 30:5419–5454. https://doi.org/10.1175/JCLI-D-16-0758.1

Giles DM, Sinyuk A, Sorokin MG, et al. (2019) Advancements in the Aerosol Robotic Network (AERONET) Version 3 database – automated near-real-time quality control algorithm with improved cloud screening for Sun photometer aerosol optical depth (AOD) measurements. Atmos Meas Tech 12:169–209. https://doi.org/10.5194/amt-12-169-2019

Hersbach H, Bell B, Berrisford P, et al. (2020) The ERA5 global reanalysis. Q J R Meteorol Soc 146:1999–2049. https://doi.org/10.1002/qj.3803

Hsu NC, Lee J, Sayer AM, Kim W, Bettenhausen C, Tsay SC (2019) VIIRS Deep Blue aerosol products over land: extending the EOS long-term aerosol data records. J Geophys Res Atmos 124:4026–4053. https://doi.org/10.1029/2018JD029688

Kaiser JW, Heil A, Andreae MO, et al. (2012) Biomass burning emissions estimated with a global fire assimilation system based on observed fire radiative power. Biogeosciences 9:527–554. https://doi.org/10.5194/bg-9-527-2012

Knapp KR, Kruk MC, Levinson DH, Diamond HJ, Neumann CJ (2010) The International Best Track Archive for Climate Stewardship (IBTrACS): unifying tropical cyclone data. Bull Am Meteorol Soc 91:363–376. https://doi.org/10.1175/2009BAMS2755.1

Levy RC, Mattoo S, Munchak LA, Remer LA, Sayer AM, Patadia F, Hsu NC (2013) The Collection 6 MODIS aerosol products over land and ocean. Atmos Meas Tech 6:2989–3034. https://doi.org/10.5194/amt-6-2989-2013

Randles CA, da Silva AM, Buchard V, et al. (2017) The MERRA-2 aerosol reanalysis, 1980 onward. Part I: system description and data assimilation evaluation. J Clim 30:6823–6850. https://doi.org/10.1175/JCLI-D-16-0609.1

Schroeder W, Oliva P, Giglio L, Csiszar IA (2014) The New VIIRS 375 m active fire detection data product: algorithm description and initial assessment. Remote Sens Environ 143:85–96. https://doi.org/10.1016/j.rse.2013.12.008

Wheeler MC, Hendon HH (2004) An all-season real-time multivariate MJO index: development of an index for monitoring and prediction. Mon Weather Rev 132:1917–1932. https://doi.org/10.1175/1520-0493(2004)132<1917:AARMMI>2.0.CO;2